TICRA

In-flight Retrieval of Geometrical information on the Planck Telescope

RFM2

Geometry retrieval using combined HFI data and LFI beam data

Author: Per Heighwood Nielsen

December, 2015 S-1563-13

TICRA
LÆDERSTRÆDE 34 · DK-1201 COPENHAGEN K DENMARK
TELEPHONE +45 33 12 45 72 TELEFAX +45 33 12 08 80
E-MAIL ticra@ticra.com http://www.ticra.com

VAT REGISTRATION NO. DK-1055 8697
TICRA FOND, CVR REG. NO. 1055 8697

TABLE OF CONTENTS

1. Introduction.

The present study is prepared for ESTEC under contract no. 18395/04/NL/NB, CCN no. 8.

The title of the work is

"In-flight Retrieval of Geometrical information on the Planck Telescope"

This Report presents the second combined retrieval of the possible telescope errors, RFM2, for the measured LFI main beams, which were deconvoluted and investigated in Report S-1563-09, and the HFI main beams, which were presented and investigated in Report S-1563-05. These HFI beams were found to be more accurate than the new beams in Report S-1563-11.

The Planck telescope is modelled as the in-Flight configuration at operational temperature as described in TICRA Report S-1531-02 and with the new detector positions, NRFFM, described in Report S-1563-09.

The geometric information is retrieved using the extended version of the Physical Optics Shaping program, POS, explained in TICRA Report S-1487-04.

2. Combined LFI and HFI Retrieval.

The retrieval is performed with the extended version of the POS program using the 22 measured LFI beams as in Report S-1563-09 and the eight outmost HFI beams from Report S-1563-05.

Zernike modes up to (3,3) on both sub- and main-reflector and a rotation of the RDP coordinate system shown in Figure 2-1 are used in the retrieval.

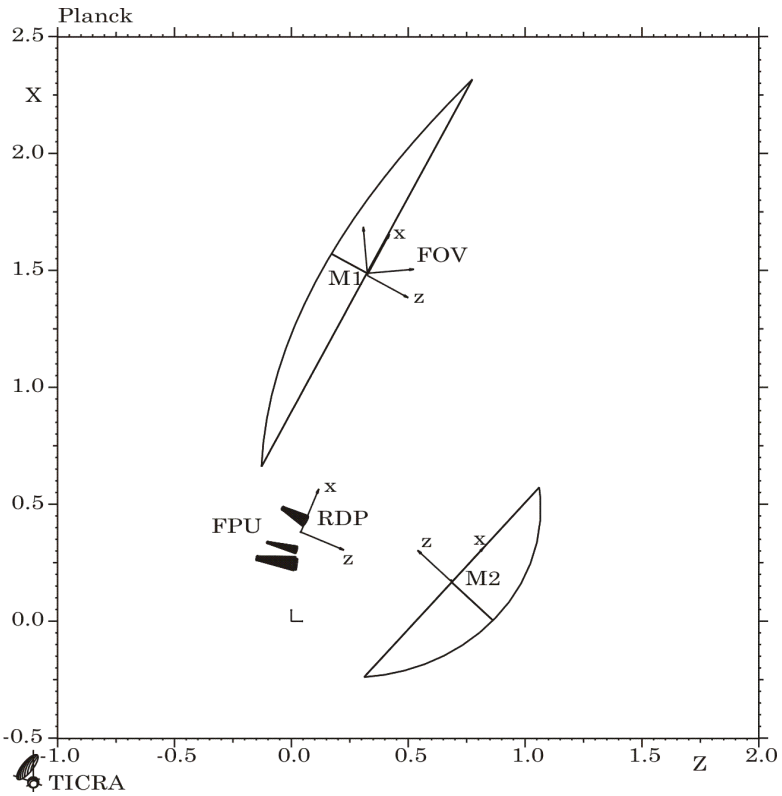

Figure 2-1 Coordinate systems in retrievals.

Using the LFI retrieved telescope geometry from Report S-1563-09 the HFI detector positions are retrieved first giving the correct beam directions in this configuration. A combined retrieval of the new mirror deformations is then performed using all fixed these detector positions.

The mirror surface distortions found in this new combined retrieval, RFM2, are shown in Table 2-1 and Table 2-2.

Zernike mode		Amplitude	Rotation
m	n	[mm]	[degrees]
0	0	0.	0
0	2	-0.08	0
1	1	0.99	68
2	2	0.13	79
1	3	0.09	6
3	3	0.06	-58

Table 2-1 Retrieved Zernike modes on main reflector.

Zernike mode		Amplitude	Rotation
m	n	[mm]	[degrees]
0	0	0.	0
0	2	0.00	0
1	1	1.37	-35
2	2	0.05	-69
1	3	0.29	-7
3	3	0.03	4

Table 2-2 Retrieved Zernike modes on subreflector.

The Zernike mode (1,1) is a result of a tilt of the sub- and main-reflectors of 10 arcmin and 4.4 arcmin, respectively, which mainly creates the overall output direction. The retrieved Zernike distorted surfaces without the large Zernike mode (1,1) are shown in Figure 2-2 and Figure 2-3 for main and sub-reflector, respectively.

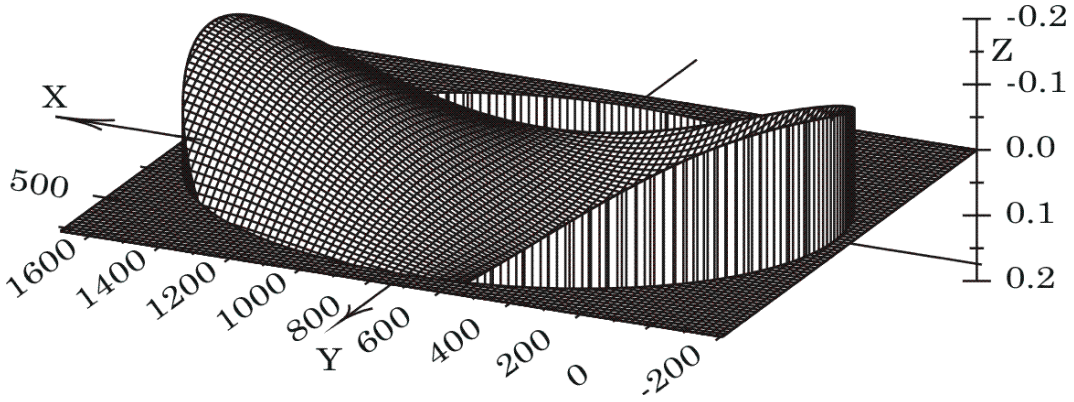

Figure 2-2 Retrieved main reflector surface deformations.

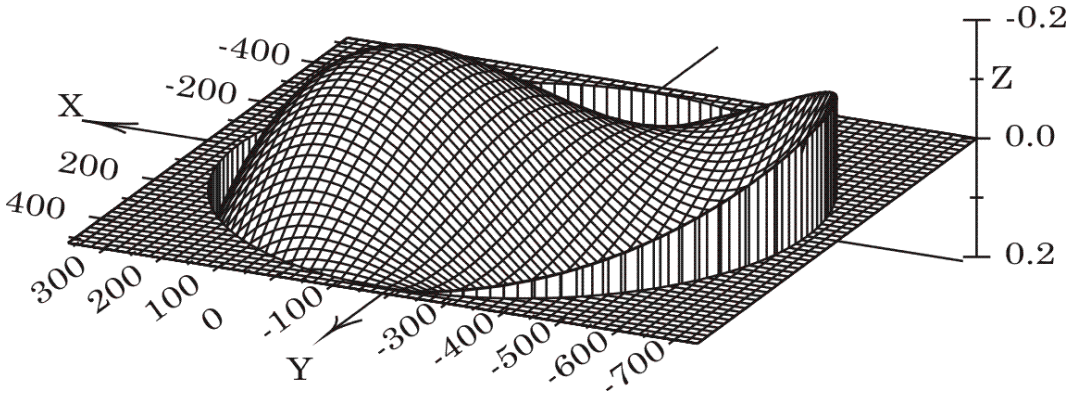

Figure 2-3 Retrieved subreflector surface deformations.

The maximum surface distortions at the rim are ±0.32 mm and ±0.20 mm for sub- and main-reflector, respectively. The large curvature on the main reflector is due to a combination of Zernike modes (0,2) and (2,2). On the subreflector it is the Zernike mode (1,3).

After this mirror retrieval the detector positions in x- and y-direction are retrieved once more for all beams. In order to reduce the maximum feed displacements a retrieval of the two different FPU coordinate systems for LFI and HFI with constraints on the possible feed displacements is performed. Again the detectors LFI20S and LFI21S are too dislocated to be used in the retrieval of the FPU for the LFI detectors.

The retrieved modifications of the LFI FPU relative to the common RDP coordinate system are:

1) translation in x-direction of ÷0.06 mm
2) translation in y-direction of ÷0.01 mm
3) translation in z-direction of +0.05 mm
4) rotation around the z-axis of ÷4.1 arcmin

The retrieved modifications of the HFI FPU relative to the common RDP coordinate system are:

1) translation in x-direction of +0.27 mm
2) translation in y-direction of ÷0.11 mm
3) translation in z-direction of +0.26 mm
4) rotation around the z-axis of +0.9 arcmin

With these FPU positions all the feed displacements are retrieved for LFI and HFI in Table 2-3 and Table 2-4, respectively. The displacements of the LFI detectors are related to the replaced feed positions in the NRRFM configuration as specified in Report S-1563-09.

Feed displacements	Deviation from retrieved RDP	
Detector	Δx [mm]	Δy [mm]
LFI-70-18	0.03	0.11
LFI-70-19	0.08	-0.13
LFI-70-20	0.16	0.34
LFI-70-21	-0.43	-0.36
LFI-70-22	0.06	0.08
LFI-70-23	0.15	0.00
LFI-44-24	-0.20	-0.16
LFI-44-25	-0.10	-0.05
LFI-44-26	0.03	0.03
LFI-30-27	-0.14	0.10
LFI-30-28	-0.04	0.09

Table 2-3 Final retrieved LFI feed displacements.

Displacements	Deviation from RDP	
Detector	Δx [mm]	Δy [mm]
HFI-100-1a	-0.04	0.00
HFI-100-4a	-0.11	0.07
HFI-143-5	0.00	-0.05
HFI-143-7	-0.04	-0.12
HFI-217-1	0.04	0.04
HFI-217-3	0.05	0.14
HFI-353-1	0.09	0.02
HFI-353-8	-0.03	-0.01
Average	0.00	0.01

Table 2-4 Final retrieved HFI feed displacements.

Due to the averaging, the LFI translation limits are now reduced to ±0.17 mm in x-direction and ±0.13 mm in y-direction for all the detectors except for the misplaced LFI20 and LFI21. The HFI translation limits are reduced to ±0.10 mm in x-direction and ±0.13 mm in y-direction

The resultant remaining beam variances down to the 15 dB level for LFI and down to 20 dB for HFI are listed in Table 2-5 and Table 2-6. The total variance for all LFI beams is 0.13 dB and for the used HFI beams 0.38 dB.The larger variance of the HFI retrieved beams is a consequence of the LFI beams preference.

	Variance δ [dB]	
Detector	S-pol	M-pol
LFI-70-18	0.08	0.08
LFI-70-19	0.10	0.15
LFI-70-20	0.15	0.16
LFI-70-21	0.17	0.15
LFI-70-22	0.08	0.10
LFI-70-23	0.10	0.10
LFI-44-24	0.10	0.07
LFI-44-25	0.13	0.17
LFI-44-26	0.10	0.19
LFI-30-27	0.13	0.10
LFI-30-28	0.14	0.12
Total	0.13 dB	

Table 2-5 Remaining LFI variances from retrieval of reflector surface distortions and feed displacement.

Detector	Variance δ [dB]
HFI-100-1a	0.21
HFI-100-4a	0.19
HFI-143-5	0.52
HFI-143-7	0.43
HFI-217-1	0.36
HFI-217-3	0.39
HFI-353-1	0.41
HFI-353-8	0.40
Average	0.38

Table 2-6 Remaining variances from retrieval of all reflector surface distortions and feed displacement.

A new retrieval of all the HFI detector displacements is now performed using both polarizations. The resulting displacements are shown in Table 2-7 and the remaining variances between the retrieved and the measured HFI fields are given in Table 2-8.

Displacements	Deviation from RDP	
Detector	Δx [mm]	Δy [mm]
HFI-100-1	-0.05	0.00
HFI-100-2	-0.05	0.08
HFI-100-3	-0.02	0.09
HFI-100-4	**-0.12**	0.09
HFI-143-1	0.01	-0.01
HFI-143-2	0.02	-0.09
HFI-143-3	0.01	-0.08
HFI-143-4	0.01	-0.08
HFI-143-5	0.00	-0.05
HFI-143-6	-0.02	-0.11
HFI-143-7	-0.04	**-0.12**
HFI-217-1	0.04	0.04
HFI-217-2	0.05	0.09
HFI-217-3	0.05	0.14
HFI-217-4	-0.04	0.23
HFI-217-5	0.08	0.07
HFI-217-6	0.03	0.00
HFI-217-7	0.00	0.11
HFI-217-8	0.06	**0.11**
HFI-353-1	0.09	0.02
HFI-353-2	0.07	-0.07
HFI-353-3	0.09	0.03
HFI-353-4	0.10	0.01
HFI-353-5	**0.11**	0.06
HFI-353-6	0.09	0.05
HFI-353-7	0.06	0.01
HFI-353-8	-0.03	-0.01
Average	0.02	0.02

Table 2-7 Retrieved HFI feed displacements.

Beam fit	Residues in dB	
Detector	a-pol	b-pol
HFI-100-1	0.21	0.23
HFI-100-2	0.27	0.25
HFI-100-3	0.26	0.25
HFI-100-4	0.19	0.19
HFI-143-1	0.51	0.53
HFI-143-2	0.38	0.39
HFI-143-3	0.46	0.43
HFI-143-4	0.64	0.63
HFI-143-5	0.52	
HFI-143-6	0.40	
HFI-143-7	0.43	
HFI-217-1	0.36	
HFI-217-2	0.37	
HFI-217-3	0.39	
HFI-217-4	0.51	
HFI-217-5	0.52	0.57
HFI-217-6	0.43	0.44
HFI-217-7	0.46	0.46
HFI-217-8	0.48	0.49
HFI-353-1	0.41	
HFI-353-2	0.56	
HFI-353-3	0.69	**0.71**
HFI-353-4	0.68	0.68
HFI-353-5	**0.71**	**0.71**
HFI-353-6	0.67	0.67
HFI-353-7	0.56	
HFI-353-8	0.40	
Total	0.49	

Table 2-8 Remaining HFI beam variances from retrieval of reflector surface distortions and feed displacement.

4. Conclusion.

The final retrieved telescope geometry is very well within the statistical and conceivable deformations. The resulting mirror surface deformations found are below ±0.3 mm and the feed positions are found to be within ±0.1 mm for all the HFI detectors and less than ±0.2 mm for the LFI detectors. The retrieved feed dislocations are mainly due to the measured individual beam pointing. However, the two most misaligned feeds, LFI20 and LFI21, may have been misplaced under FPU assembling.

The 0.3 mm large translation of all the HFI feeds in the x-direction of the RDP coordinate system is due to the difference of 0.9 arcmin in average beam directions in cx-scan direction between the LFI and HFI.

The remaining differences between the retrieved and the measured beams, see Table 2-6 and Table 2-8, may be due to measurement noise and inaccuracies in the beam directions, especially for the HFI beams. The retrieval is also dependent on the calculated patterns from the detectors. The LFI detectors are conventional RF horns which are highly accurate and tested, whereas the HFI detectors are advanced and shaped horns with filter sections and bolometers.

The main difference between this retrieval, RFM2, and the first retrieval, RFM1, is the absent z-translation of the mirrors. These translations were shown in Report S-1563-12 to be unimportant and correlated with the first Zernike modes. Also the z-translation of the FPU positions is changed significantly from -.8 mm to around 0.1 mm only. The main reason for this is the misplacement of the LFI detectors which was found and has now been corrected in the NRFFM telescope geometry.

The remaining variance in Table 2-5 of the LFI beams is slightly smaller than the obtained variances in RFM1, see Table 3-13 in Report S-1563-07. Especially the variance of the LFI-70-18S beam is reduced from 0.21 dB to 0.08 dB. This is a consequence of the smaller influence of the HFI beams in the retrieval. Due to the cleaning of the HFI beams for noise and signal deformities the obtained stacked beams are found to be more unreliable than the LFI beams. Therefore, this final retrieval is based on a separate geometrical retrieval of the mirrors using the LFI beams only and a starting position of HFI detectors fine-tuned to this geometry. Therefore, the averaged HFI variance is increased from 0.3 dB in RFM1 to 0.5 dB.

References

P. Nielsen, 2009
"In-flight Retrieval of Geometrical information on the Planck Telescope – Retrieval of geometrical information and evaluation of results", S-1487-04, dated February 2009.

P. Nielsen, 2010
"In-flight Retrieval of Geometrical information on the Planck Telescope – Evaluation of weight influence", S-1531-02, dated March 2010.

P. Nielsen, 2010
"In-flight Retrieval of Geometrical information on the Planck Telescope – LFI Smearing effect on alignment retrieval", S-1531-07, dated October 2010.

P. Nielsen, 2013
"In-flight Retrieval of Geometrical information on the Planck Telescope – HFI optical beam data with IMO 1731634056801705766", S-1563-05, dated April 2013.

Fabrizio Villa, 2014
"LFI phase centre horn positions", e-mail correspondence, March 25, 2014.

P. Nielsen, 2014
"In-flight Retrieval of Geometrical information on the Planck Telescope – Geometry retrieval using LFI beam data from all Jupiter scans", S-1563-09, dated September 2014.

P. Nielsen, 2015
"In-flight Retrieval of Geometrical information on the Planck Telescope – Geometry retrieval using new HFI beam data from all Saturn scans", S-1563-11, dated June 2015.

P. Nielsen, 2015
"In-flight Retrieval of Geometrical information on the Planck Telescope – Alternative Geometry retrieval using LFI beam data from all Saturn scans", S-1563-12, dated June 2015.

A. Least Squares Optimization Residue

The residual function for the least squares optimization is defined as

$$f_{bi}(\overline{x}) = w_b w_i (d_{meas,i} - d_i(\overline{x}) - \mu_b) = w_b w_i (\Delta_i(\overline{x}) - \mu_b)$$

With the following parameters

b the subscript referring to each beam

i subscript referring to the signal index in each beam

$\overline{x}$ the vector holding all variables involved in the optimization

w_b the individual beam weight factor calculated from the noise levels in dB below peak, N_{bp}: $w_b = 10^{(N_{bp}/10)}$

w_i the weight factor given as the square root of the measured beam power and with the maximum power for each beam b, $d_{meas,\max,b}$, normalized to 1.

$$w_i = \sqrt{d_{meas,i} \,/\, d_{meas,\max,b}}$$

$d_{meas,i}$ the measured un-normalized signal power (temperature) given in dB in measurement index i

$d_i(\overline{x})$ the calculated 4π normalized power (directivity) of the current retrieved telescope configuration given in dBi at signal direction i.

$\Delta_i(\overline{x})$ the difference: $\Delta_i(\overline{x}) = d_{meas,i} - d_i(\overline{x})$

μ_b the weighted mean value in dB for beam b, see Figure A-1, with N_b beam signals is given by

$$\mu_b = \sum_{i=1}^{N_b} (w_i{}^2 \Delta_i)) \,/\, \sum_{i=1}^{N_b} w_i{}^2)$$

The squared variance to be minimized then is

$$\delta^2 = \sum_{b=1}^{B} \frac{1}{N_b} \sum_{i=1}^{N_b} f_i{}^2 \,/\, \sum_{b=1}^{B} (\frac{w_b{}^2}{N_b} \sum_{i=1}^{N_b} w_i{}^2)$$

Only measurement values where the power is above a specific level are used in the summation. The weights and the number of signals are given in Table A-1.

LFI		
Detector	Weight w_b	N_{bp}
LFI27S	25.12	7667
LFI28S	25.12	7686
LFI24S	39.81	6475
LFI25S	25.12	9620
LFI26S	25.12	9226
LFI18S	79.43	4535
LFI23S	63.10	4076
HFI		
Detector	Weight w_b	N_{bp}
HFI_100_1a	100.00	7746
HFI_100_4a	100.00	7466
HFI_143-5	100.00	4701
HFI_143-7	100.00	4479
HFI_217-1	100.00	1968
HFI_217-3	100.00	1807
HFI_217-4	100.00	1979
HFI_353-1	100.00	1975
HFI_353-8	100.00	2008

Table A-1 Weights in retrieval.

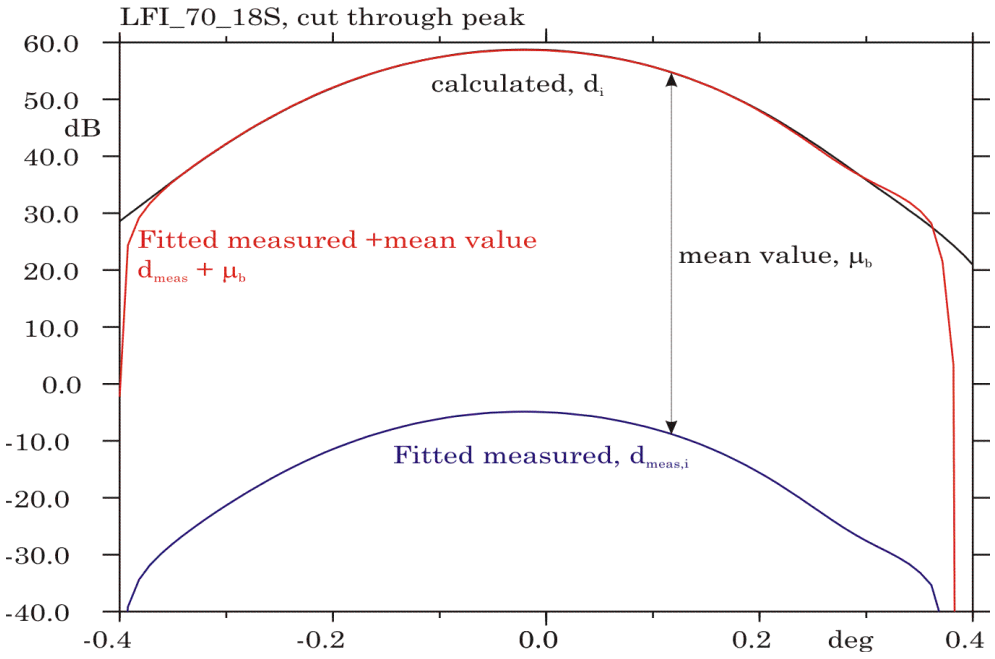

Figure A-1 Level difference between measured pattern and normalized calculated pattern.